Interrogation Modalities and Benefits of 3-Dimensional Reconstruction in Weld Characterization

SAND2011-7693C

Jonathan D. Madison, Ph.D.

SNL, Computational Material Science & Engineering, Albuquerque, NM

LOCKHEED MARTIN

Sandia National Laboratories

NNSA

Sandia National Laboratories is a multi-program laboratory managed and operated by Sandia Corporation, a wholly owned subsidiary of Lockheed Martin Corporation, for the U.S. Department of Energy's National Nuclear Security Administration under contract DE-AC04-94AL85000.

Acknowledgements

- Sandia National Laboratories, Albuquerque, NM
  - Danny O. Maccallum, Org. 1831 – Multiscale Metallurgical S&T
  - Joseph A. Romero, Org. 1522 – Experimental NDE & Model Validation
  - Burke L. Kernen, Org. 1522 – Experimental NDE & Model Validation
  - Kevin D. Rolfe, Org. 1522 – Experimental NDE & Model Validation
  - Alice Kilgo, Org. 1822 – Materials Characterization
  - Bethany N. Lust, Org. 1814 – Computational Materials Science & Engineering

- University of Michigan
  - Larry K. Aagesen, Ph.D., Post-Doc – Materials Science & Engineering

- Sandia National Laboratories, Early Career LDRD Award

Laboratory Directed Research & Development

Outline

- Background
  - Sandia History; Evolving Mission; People; Disciplines & Thrusts
  - 3-Dimensionality (Characterization & Modeling)
- Interrogation Methods (Benefits & Challenges)
  - Length Scale
  - Destructive/Non-Destructive
  - Labor Intensity
  - Data Acquisition Time
- Weld Characterization
  - Mechanical Sectioning
  - Ultrasonic Scan
  - Micro-Computed Tomography
- Summary
- Future Work

Sandia's History

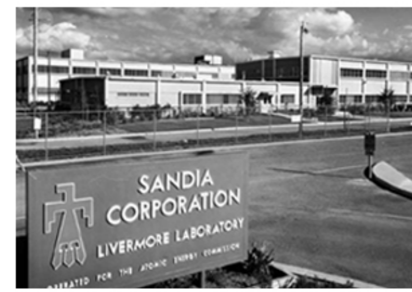

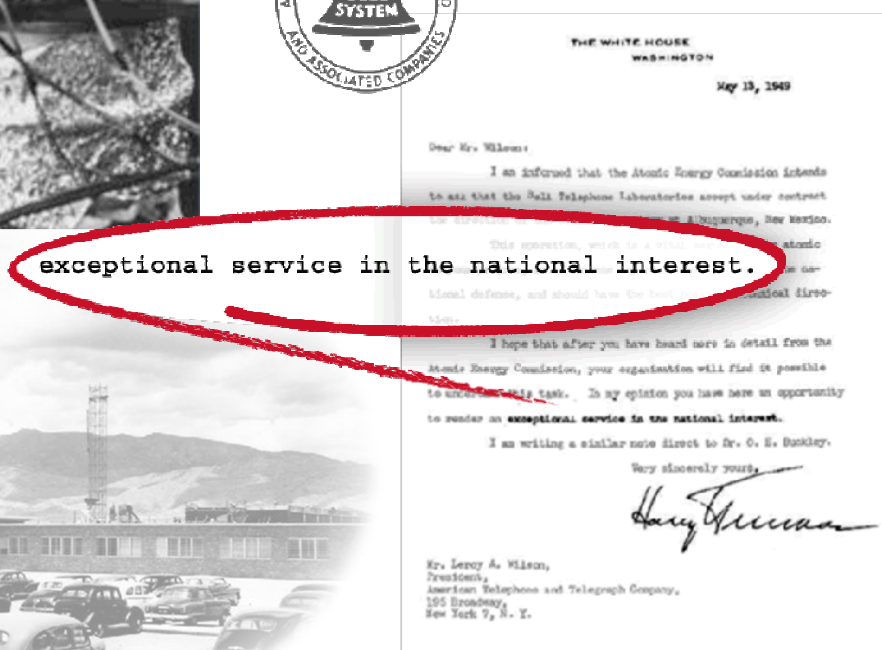

THE WHITE HOUSE
WASHINGTON

May 13, 1949

Dear Mr. Wilson:

I am informed that the Atomic Energy Commission intends to ask that the Bell Telephone Laboratories accept under contract the direction of [illegible] at Albuquerque, New Mexico.

This operation, which is a vital [illegible] atomic [illegible] national defense, and should have the best [illegible] technical direction.

I hope that after you have heard more in detail from the Atomic Energy Commission, your organization will find it possible to undertake this task. In my opinion you have here an opportunity to render an **exceptional service in the national interest.**

I am writing a similar note direct to Dr. O. E. Buckley.

Very sincerely yours,

Harry Truman

Mr. Leroy A. Wilson,
President,
American Telephone and Telegraph Company,
195 Broadway,
New York 7, N. Y.

Sandia National Laboratories

Sandia's Evolving Mission

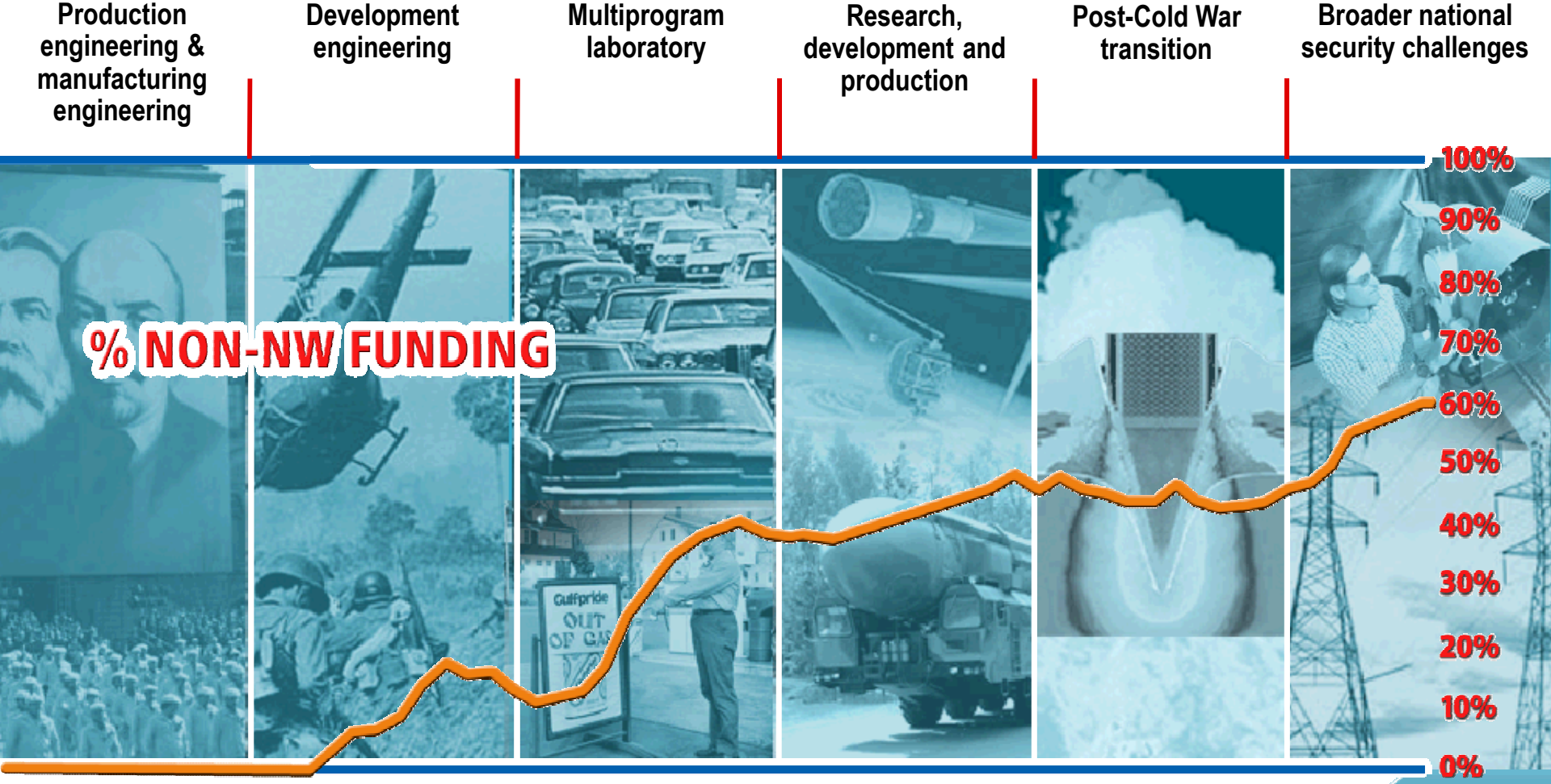

Sandia National Laboratories

People and Budget (as of 10.15.2010)

- On-site workforce: 11,677
- Regular employees: 8,607
- Gross payroll: ~ $898.7 million

FY10 operating revenue
$2.3 billion

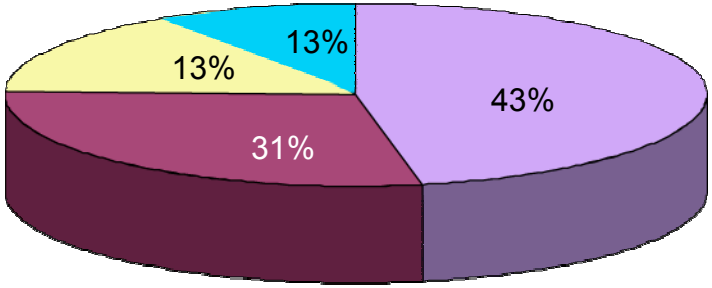

Technical staff (4,277) by discipline:

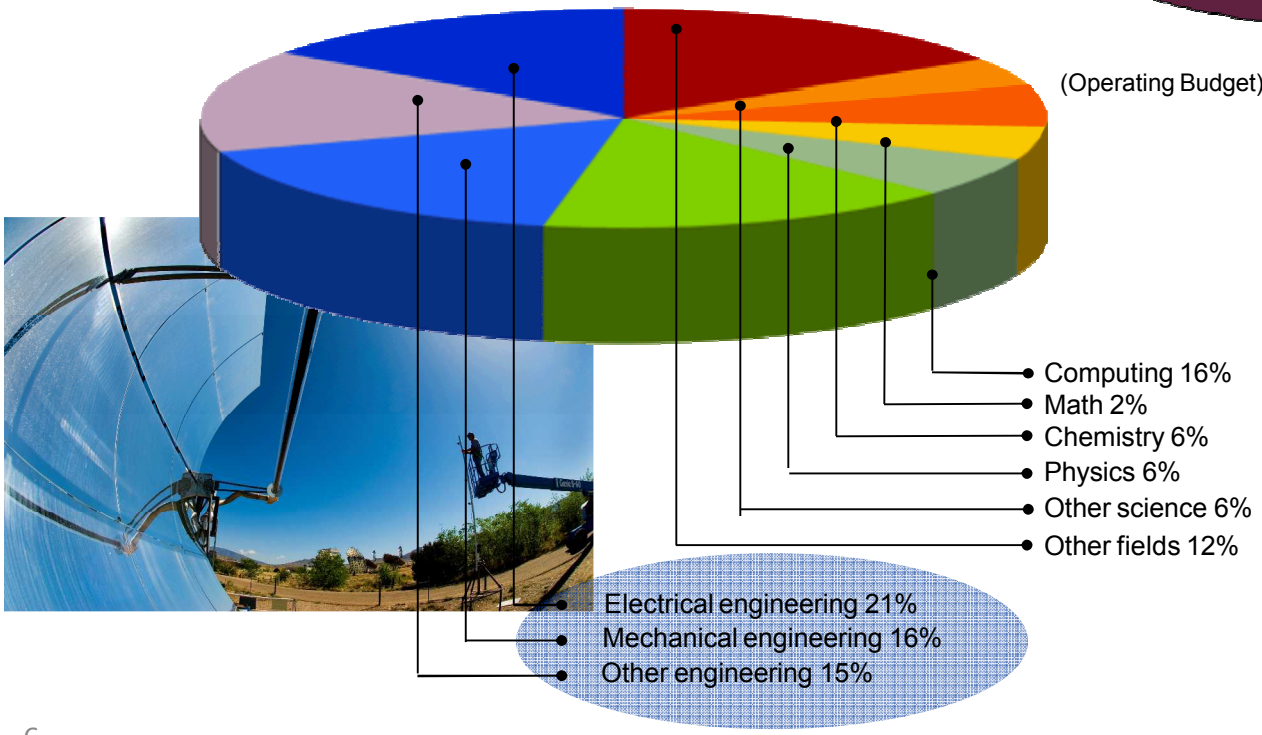

(Operating Budget)

- Nuclear Weapons
- Defense Systems & Assessments
- Energy, Climate, & Infrastructure Security
- International, Homeland, and Nuclear Security

Sandia National Laboratories

Research Disciplines & Capabilities

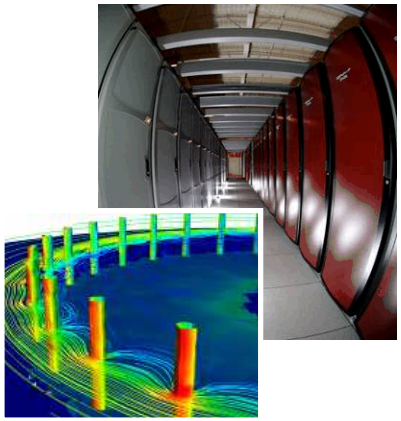

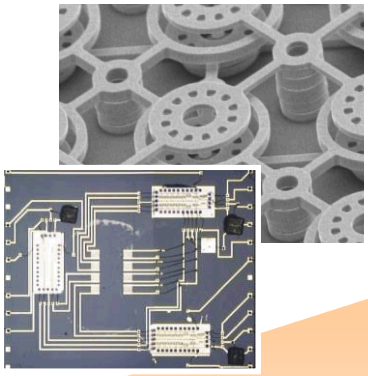

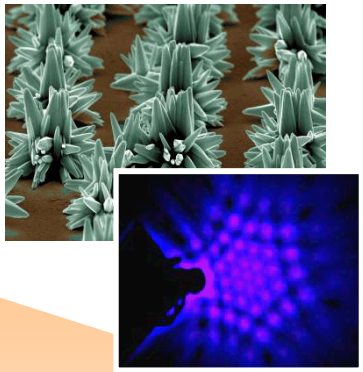

High Performance Computing

Nanotechnologies & Microsystems

Extreme Environments

COMPUTER SCIENCE | MATERIALS | ENGINEERING SCIENCES | MICRO ELECTRONICS | BIOSCIENCE | PULSED POWER

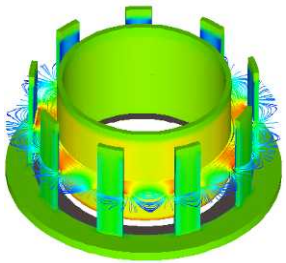

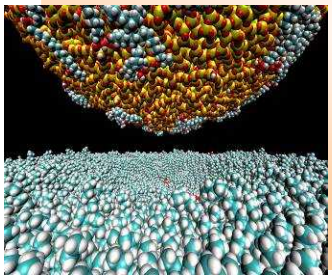

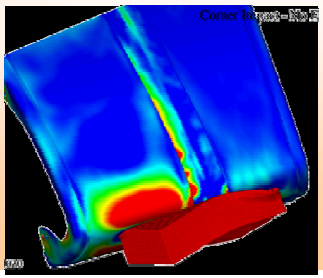

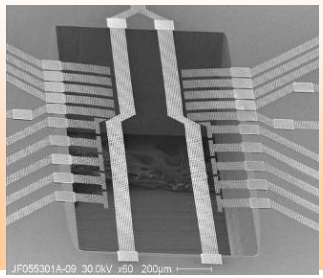

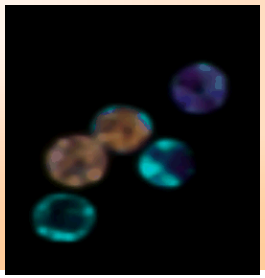

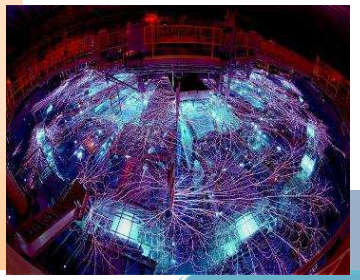

RESEARCH DISCIPLINES

Emerging National Security Thrusts

Nuclear

Energy

Cyber

Science & Technology

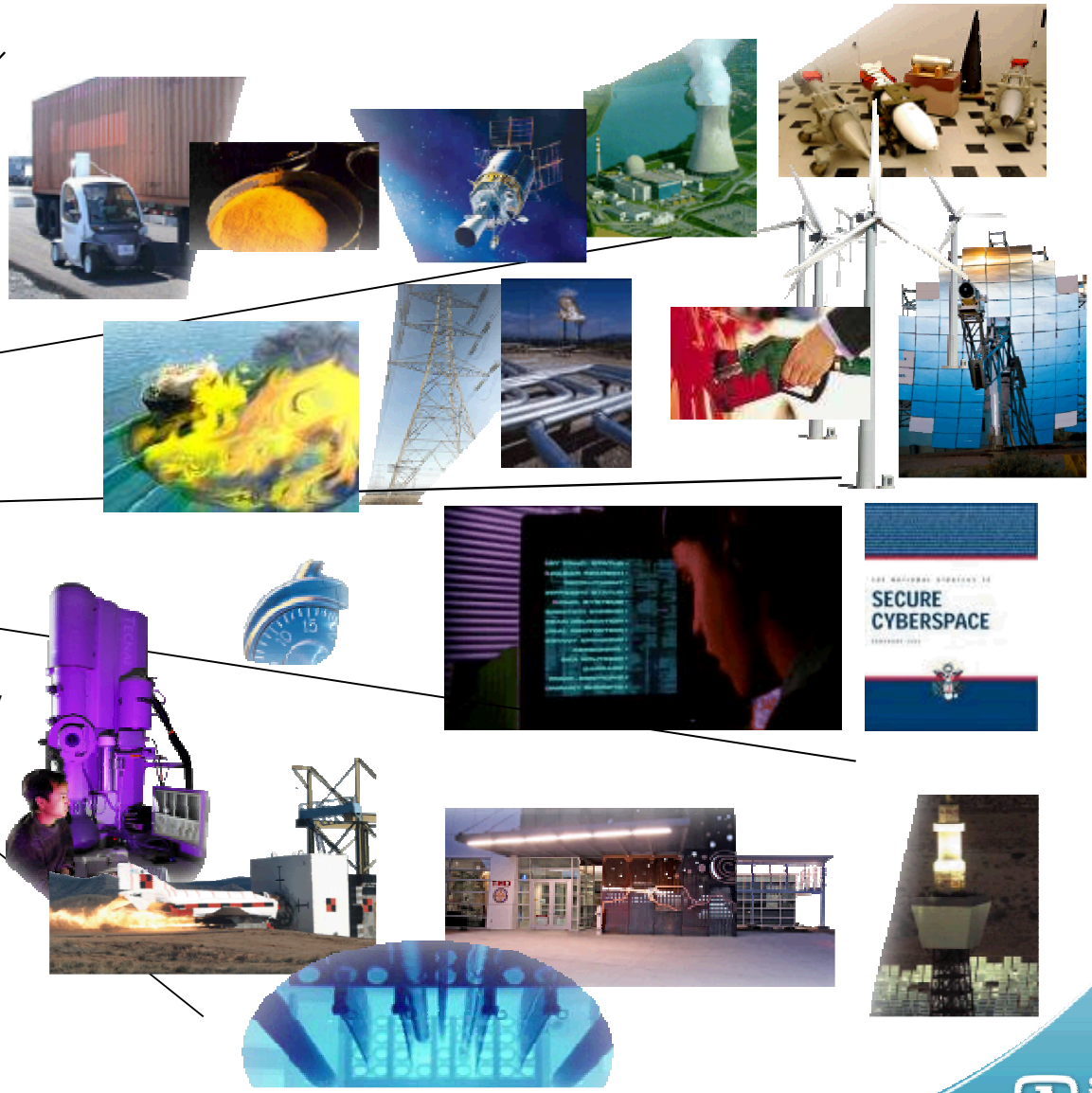

Sandia National Laboratories

3-Dimensionality

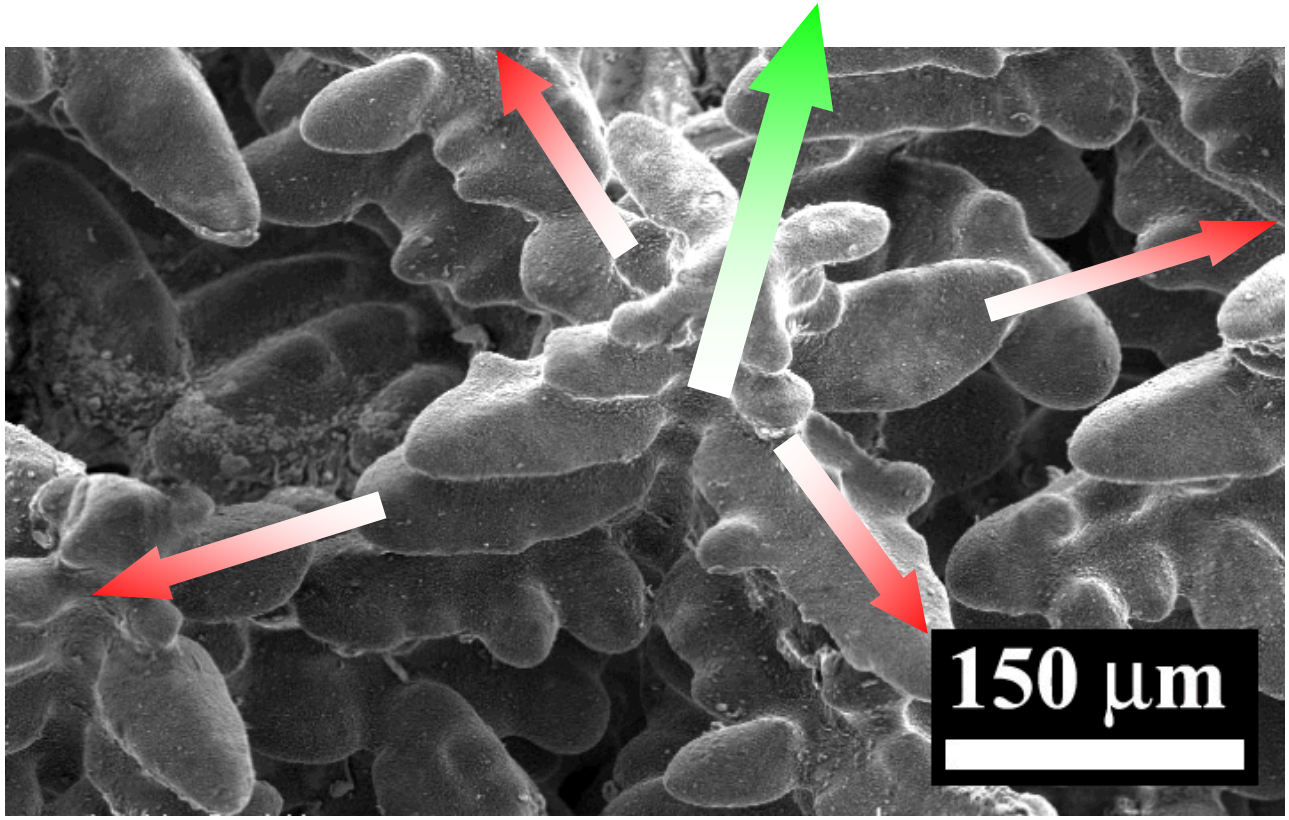

J. Madison *et al., "Fluid Flow and Defect Formation in the Three-Dimensional Dendritic Structure of Nickel-Based Single Crystals"* **METALLURGICAL & MATERIALS TRANSACTIONS A** doi: 10.1007/s11661-011-0823-8

J. Madison *et al., "Modeling Fluid Flow in Three-Dimensional Single Crystal Dendritic Structures"* **ACTA MATERIALIA** 58 (2010) pp. 2864 – 2875

9

Characterization > Modeling

Liquid Representations

Ni-Al-W Ternary

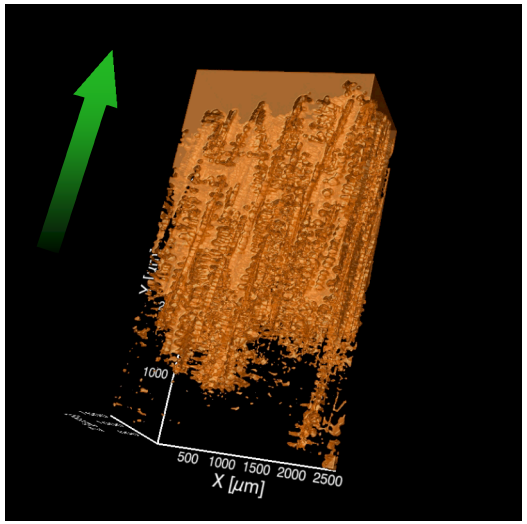

René N4

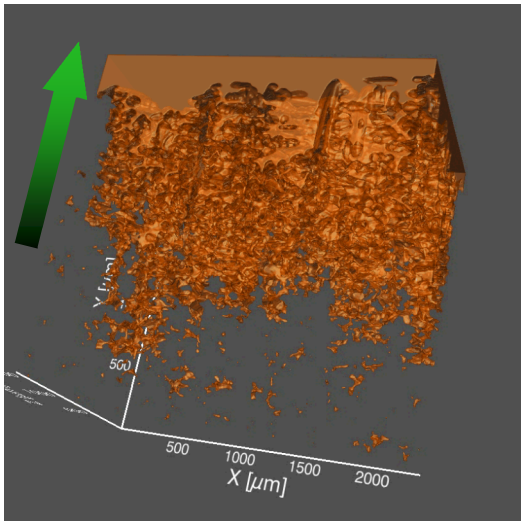

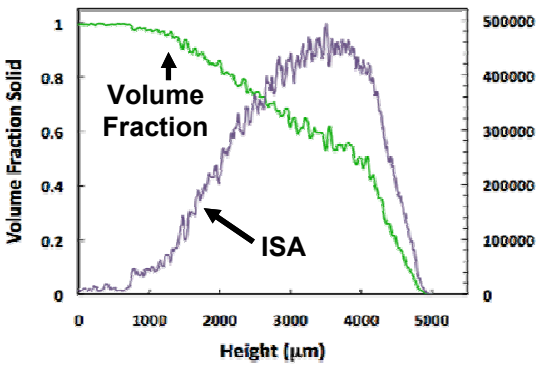

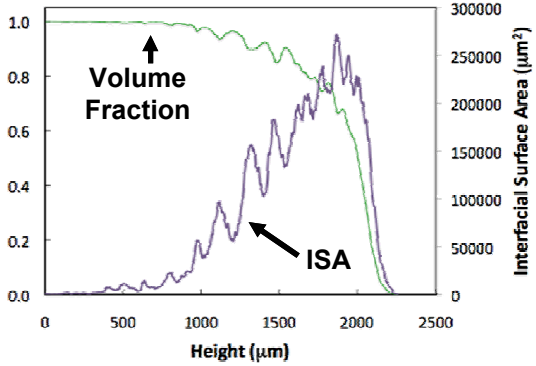

- 3D reconstructions at the dendritic front in two experimentally derived nickel-base superalloy systems
  - Characterization including direct measurement of interfacial surface area providing indication of its effect on flow
- Simulation of 3D fluid flow parallel (K_y), and normal (K_x), to the primary growth direction as functions of volume fraction.

FLUENT

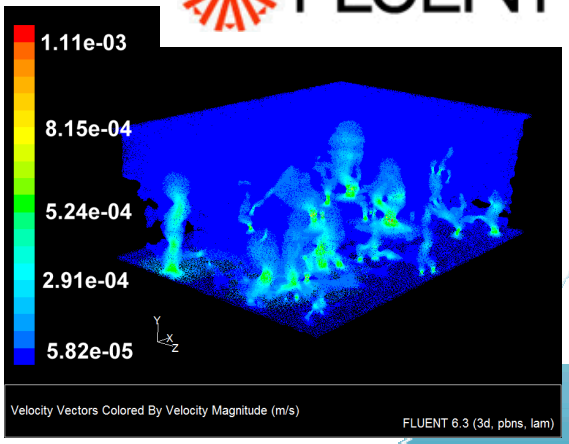

Sandia National Laboratories

Model > Predictors

$$Ra = \frac{(\Delta\rho/\rho_o)gKh}{\alpha\nu}$$

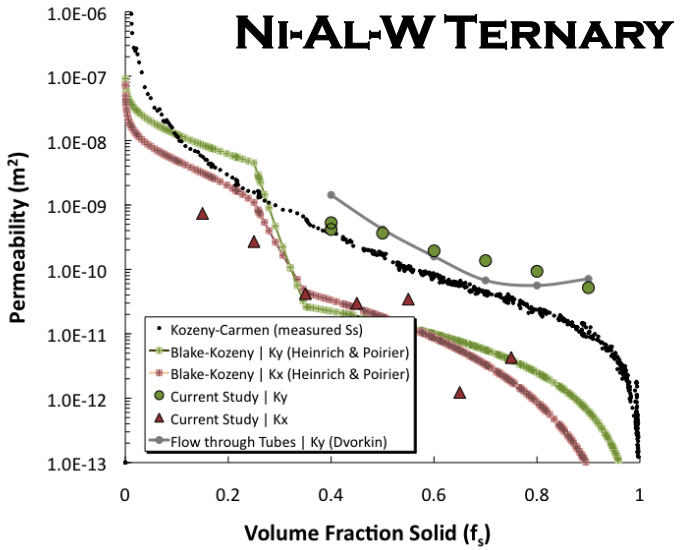

- Decreases in permeability coincide with increased tortuosity only in vertical flow (K_y)

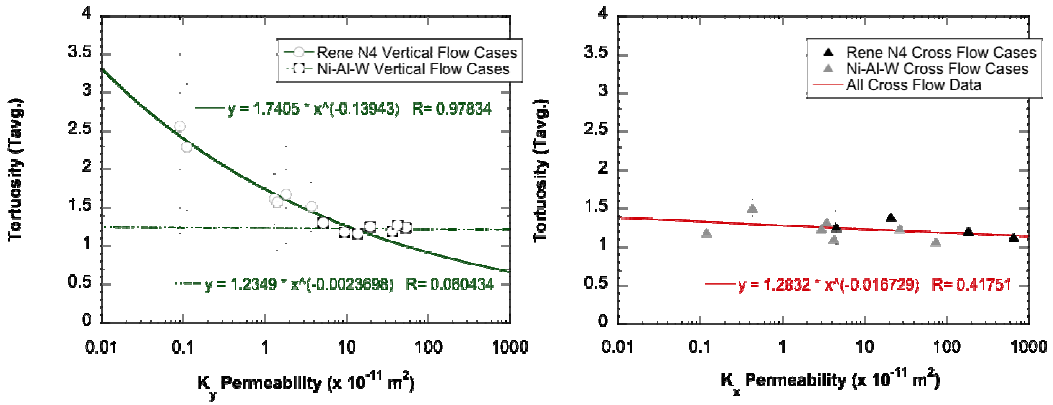

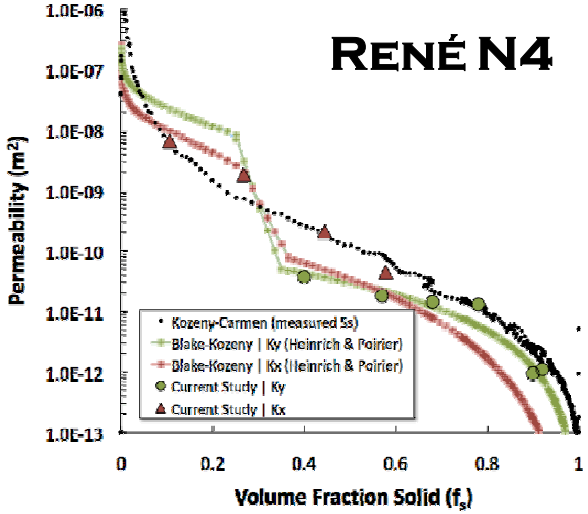

- Permeability scales inversely with S_V in both vertical and cross flow (K_y) regardless of volume fraction

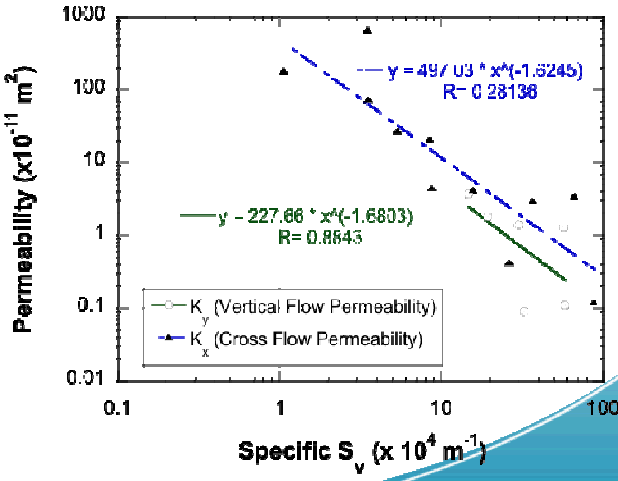

Sandia National Laboratories

Interrogation Methods

	Length scales (m)	Destructive (D/ND)	Labor Intensity	Data Acquisition Time
Atom Probe Tomography [APT]	$10^{-10} – 10^{-8}$	D	Medium	Medium
Focused Ion Beam Milling [FIB]	$10^{-8} – 10^{-5}$	D	Low	Medium
Mechanical Serial Sectioning [MS]	$10^{-7} – 10^{-3}$	D	High	High
3DXray Diffraction [3DXRD]	$10^{-6} – 10^{-3}$	ND	High	High
Micro-Computed Tomography [μCT]	$10^{-6} – 10^{-3}$	ND	Low	Low
Femto-second Laser Sectioning [FSL]	$10^{-5} – 10^{-3}$	D	Low	Low
Ultrasonic Testing Scan [UTC]	$10^{-5} – 10^{-1}$	ND	Low	Low

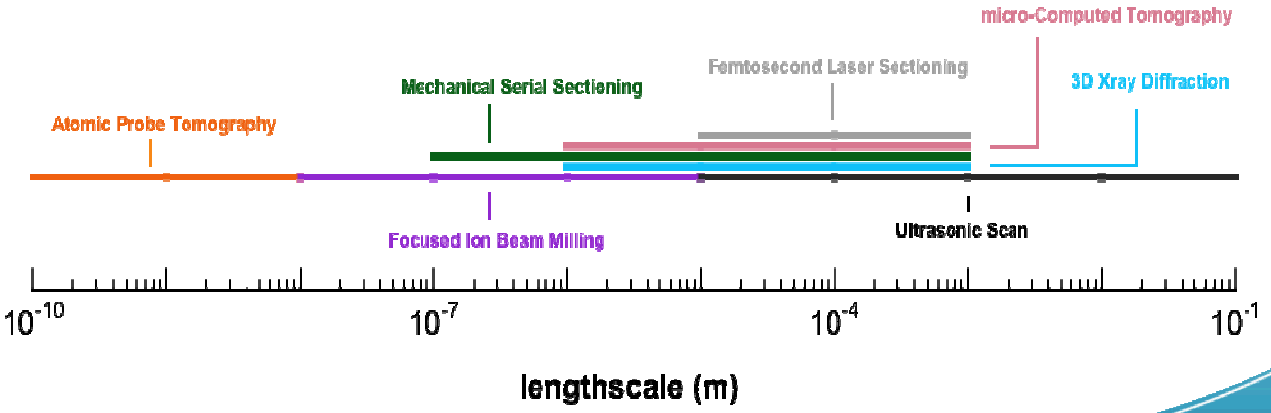

Interrogation Methods

	Obtainable Data	References
Atom Probe Tomography [APT]	*(in-situ)* material absence, elemental composition, inclusion identification	Y. Amouyal, D.N. Seidman, ***Acta Mat.,*** 2011, in press D. Isheim, ***Scripta Mater.,*** 2006, p. 35
Focused Ion Beam Milling [FIB]	*(in-situ)* material absence, crystallography, inclusion identification	M. Uchic, et al., ***Scripta Mater.,*** 2006, p. 23 M. Uchic, et al., Ultramicroscopy, 2009, p. 1229
Mechanical Serial Sectioning [MS]	material absence, crystallography, inclusion identification	J. Spowart, ***Scripta Mater.,*** 2006, p. 5 G. Spanos, et al. ***MRS Bulletin,*** 2008, p. 597
3DXray Diffraction [3DXRD]	material absence, crystallography, inclusion identification	E. Lauridsen, et al., ***Scripta Mater.,*** 2006, p. 51 D. Juul Jensen, et al., ***MRS Bulletin,*** 2008, p. 621
Micro-Computed Tomography [μCT]	material absence	J. Baruchel, et al., ***Scripta Mater.,*** 2006, p. 41 J.-Y. Buffiere et al., ***MRS Bulletin,*** 2008, p. 611
Femto-second Laser Sectioning [FSL]	material absence, crystallography, inclusion identification	M. Echlin, et al., ***Adv. Mater.***, 2011, p. 2339
Ultrasonic Testing Scan [UTC]	material absence	A.S. Birks & R.E. Green, Ultrasonic Testing (NDT Handbook) vol. 7, ASND, 1991

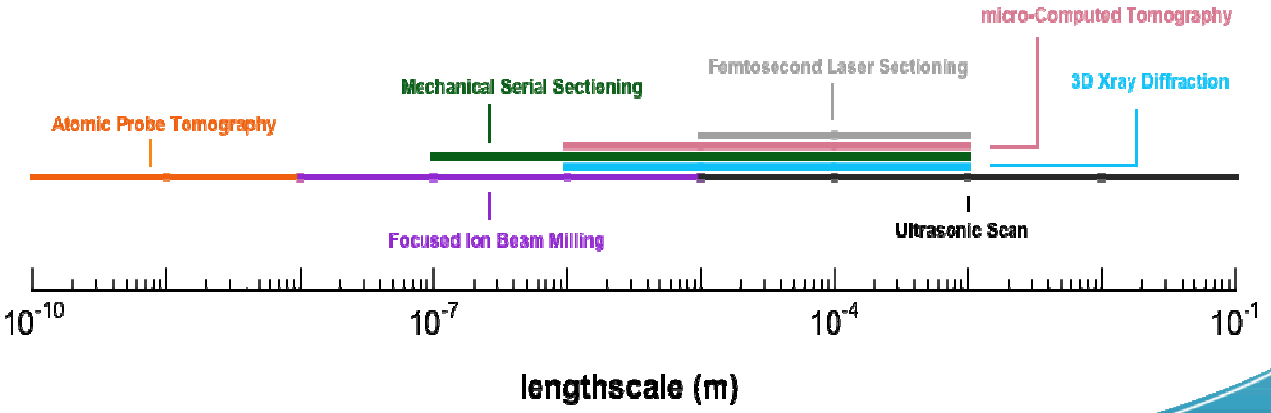

Weld Applicability to SNL

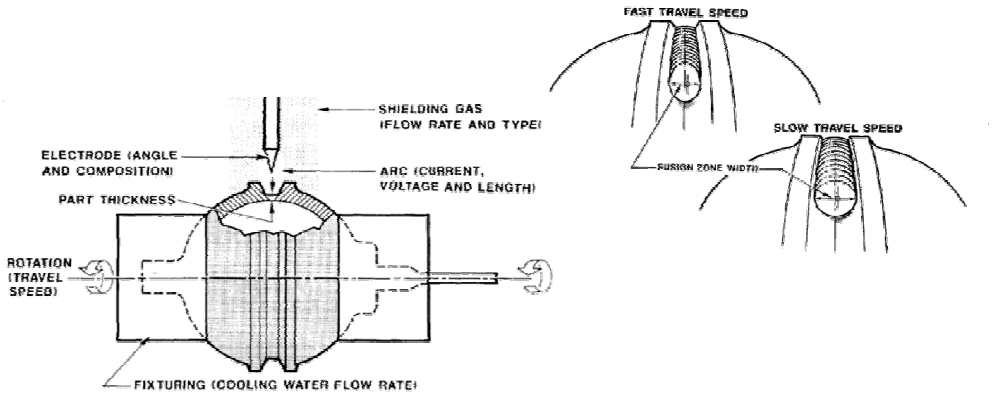

A. Bentley, **SAND2002-4014** : Feedback Control of Arc Welding Using Quantitative Feedback Theory, February 1991

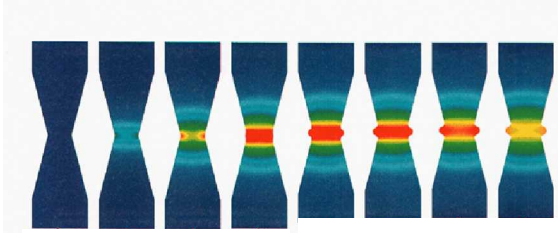

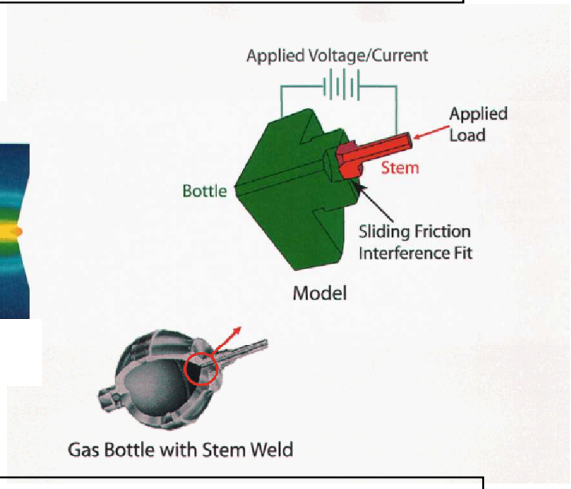

W. Winters, A. Brown, D. Bammann, J. Foulk III, A. Ortega, **SAND2005-3000:** Progress Report for the ASCI AD Resistance Weld Process Modeling Project AD2003-15, May 2005

- M. Cieslak, A. Ritter, "Precipitate Formation in Austenitic Stainless Steel Welds," Scripta Met., Vol. 19, Issue 2, (1985) pp. 165-168
- J. Jellison, M. Cieslak, *Laser Materials Processing at Sandia National Laboratories,* presented at Applications of Lasers and Electro-Optics, Orlando FL, October 1994
- J. Knorovsky, M. Kanouff, P. Fuerschbach, D. Noble, P. Schunk, D. MacCallum, Hooper, *Calculated versus experimental heat inputs in laser spot welding,* presented at The American Welding Society, Chicago IL, April 2000
- C. Robino, A. Hall, J. Brooks, T. Headley, R. Roach, **SAND2002-4014** : Solidification Diagnostics for Joining and Microstructural Simulations, January 2003
- V. Semak, G. Knorovsky, D. MacCallum, R. Roach, "Effect of Surface Tension on Melt Pool Dynamics During Laser Pulse Interaction," J. Phys. D: Appl. Phys. Vol. 39, (2006) pp. 590-595
- J. Norris, M. Perricone, R. Roach, K. Faraone & C. Ellison, **SAND2007-1051** : Evaluation of Weld Porosity in Laser Beam Seam Welds: Optimizing Continuous Wave and Square Wave Modulated Processes, February 2007

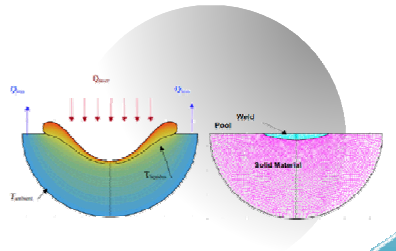

Sandia National Laboratories

Design of Experiment

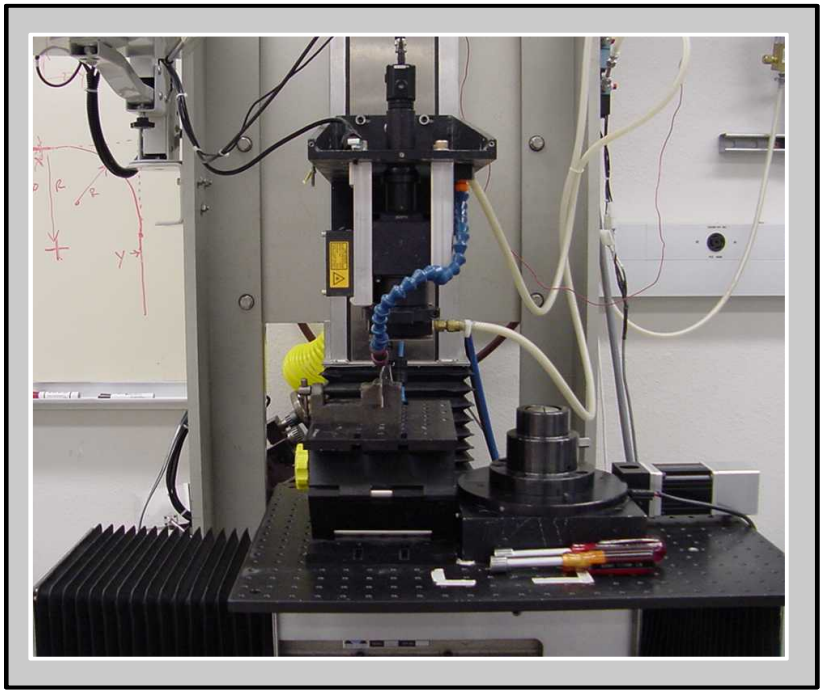

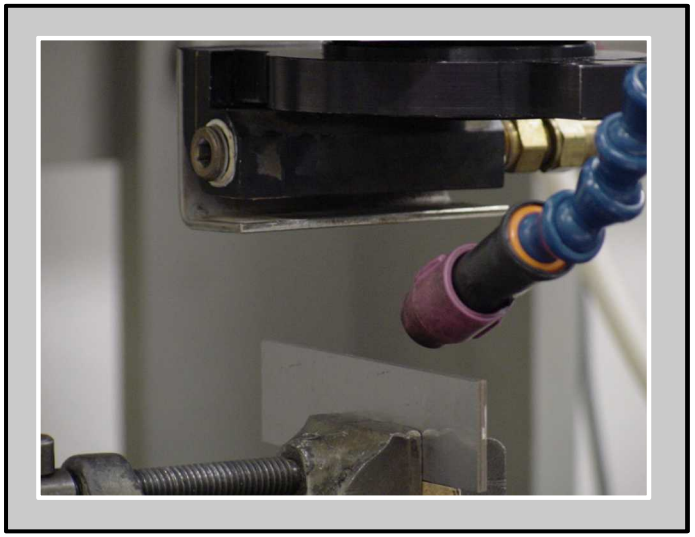

C	Cr	Mn	Ni	N	P	S	Si	Fe
0.04	18.12	1.21	8.09	0.028	0.022	0.001	0.34	bal.

304L Stainless Steel (wt%)

Quantity	Lens	Power (Measured)	Speed
(2)	80 mm	1200 W	40”/min
(2)	80 mm	1200 W	60”/min
(2)	80 mm	1200 W	80”/min
(2)	120 mm	1200 W	40”/min
(2)	120 mm	1200 W	60”/min
(2)	120 mm	1200 W	80”/min

Material:	304L Stainless Steel
Heat :	481361 (1.92 Cr/Ni)
Laser:	Rofin Nd:YAG

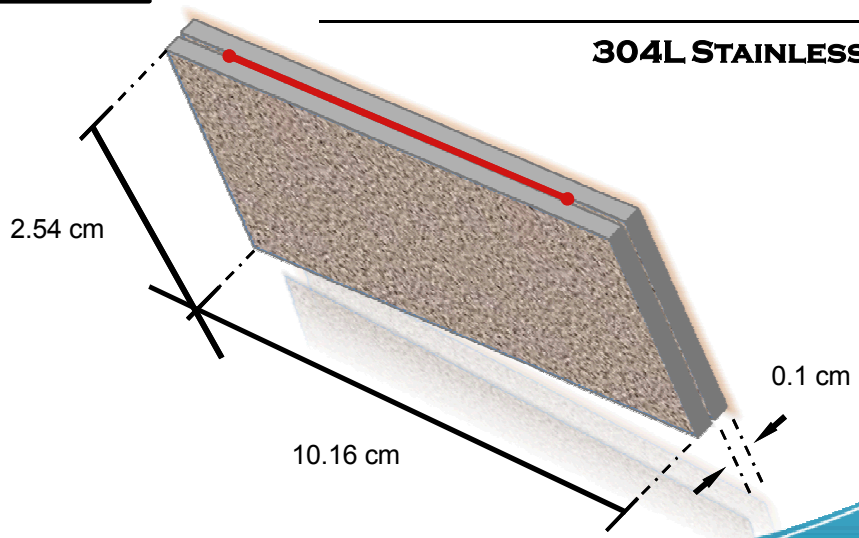

Mechanical Sectioning [MS]

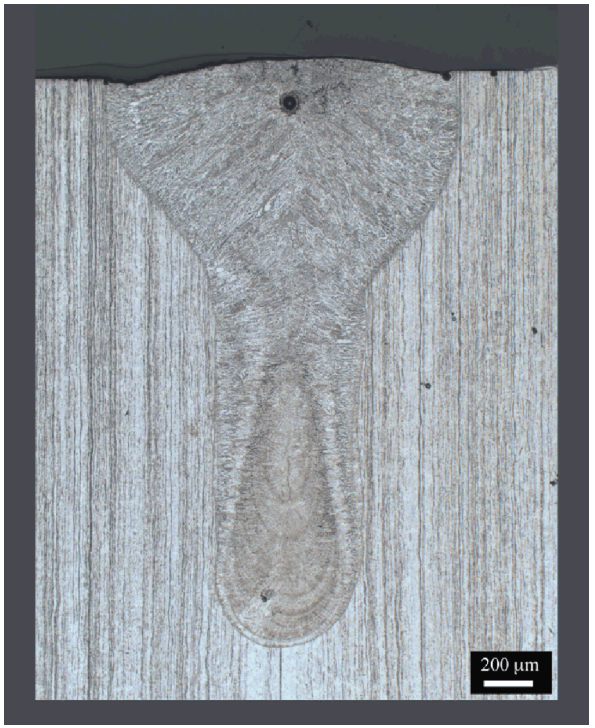

Quantity	Lens	Power (Measured)	Speed
(2)	80 mm	1200 W	40”/min
(2)	80 mm	1200 W	60”/min
(2)	80 mm	1200 W	80”/min
(2)	120 mm	1200 W	40”/min
(2)	120 mm	1200 W	60”/min
(2)	120 mm	1200 W	80”/min

Material:	304L Stainless Steel
Heat :	481361 (1.92 Cr/Ni)
Laser:	Rofin Nd:YAG

Mechanical Sectioning [MS]

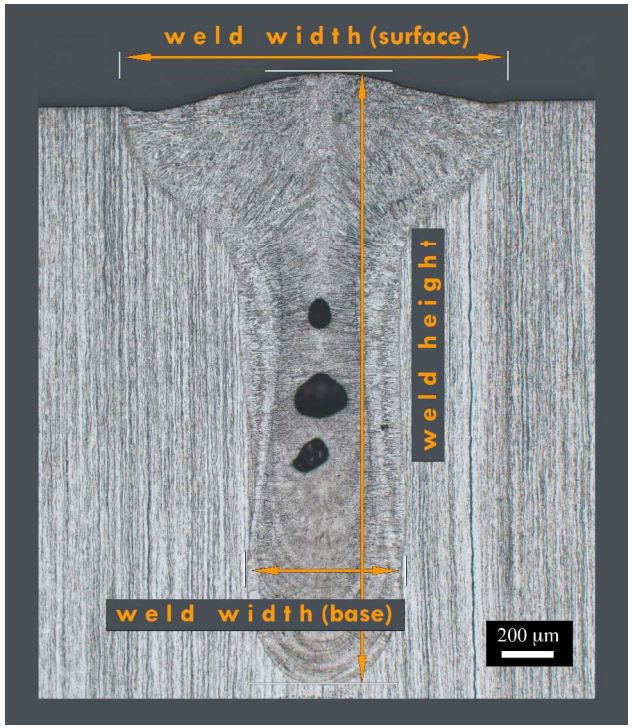

Quantity	Lens	Power (Measured)	Speed

Material:	304L Stainless Steel
Heat :	481361 (1.92 Cr/Ni)
Laser:	Rofin Nd:YAG

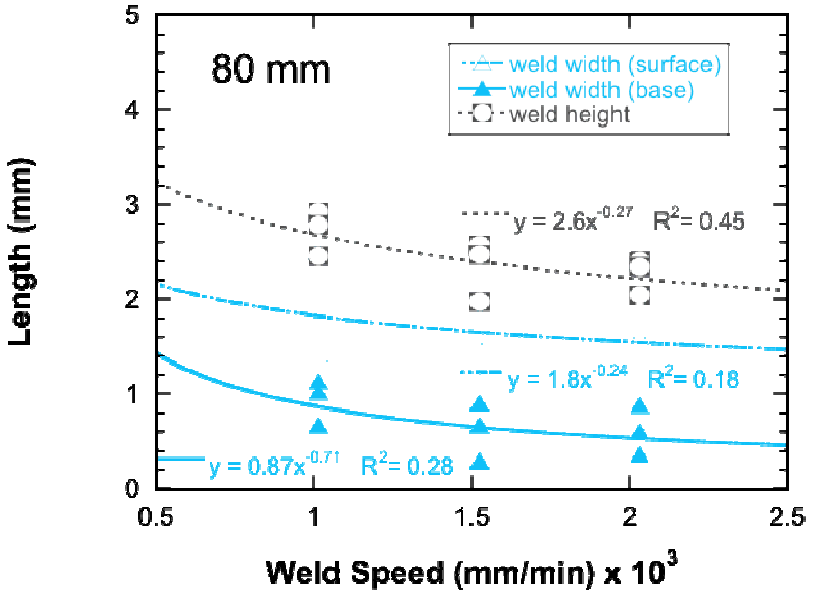

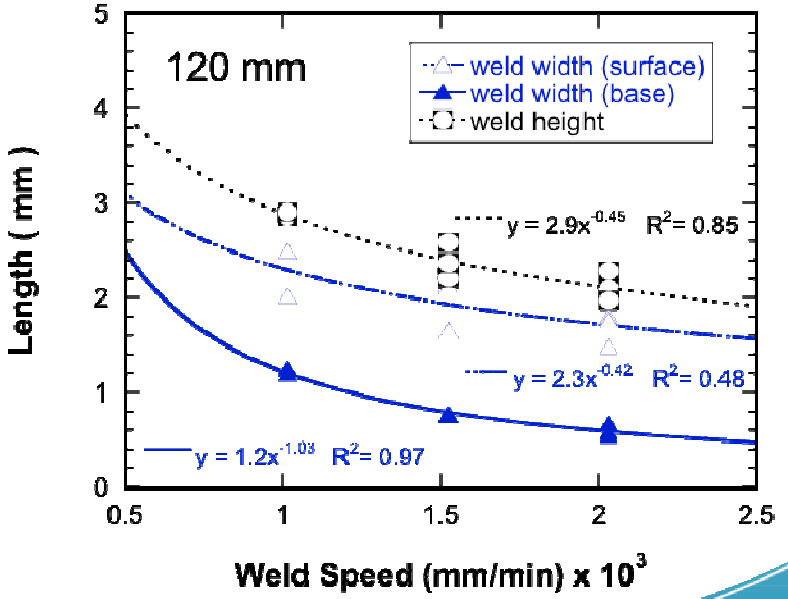

Mechanical Sectioning [MS]

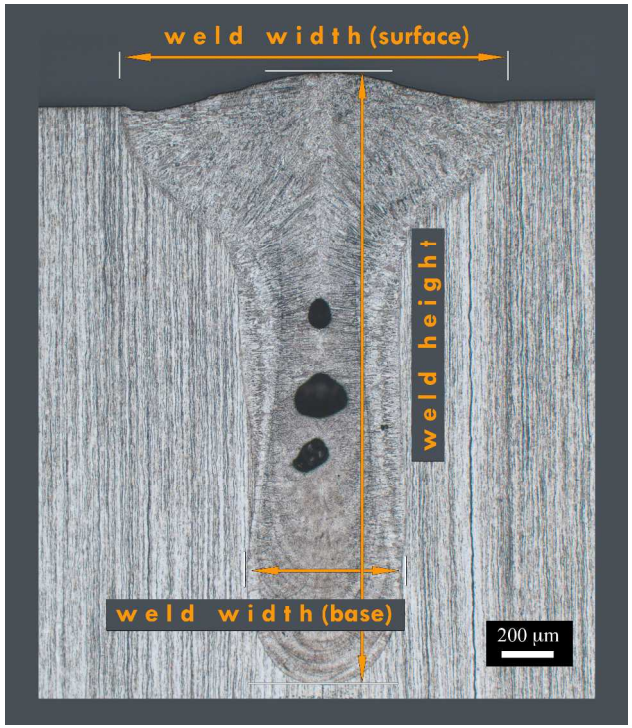

Quantity	Lens	Power (Measured)	Speed

Material:	304L Stainless Steel
Heat :	481361 (1.92 Cr/Ni)
Laser:	Rofin Nd:YAG

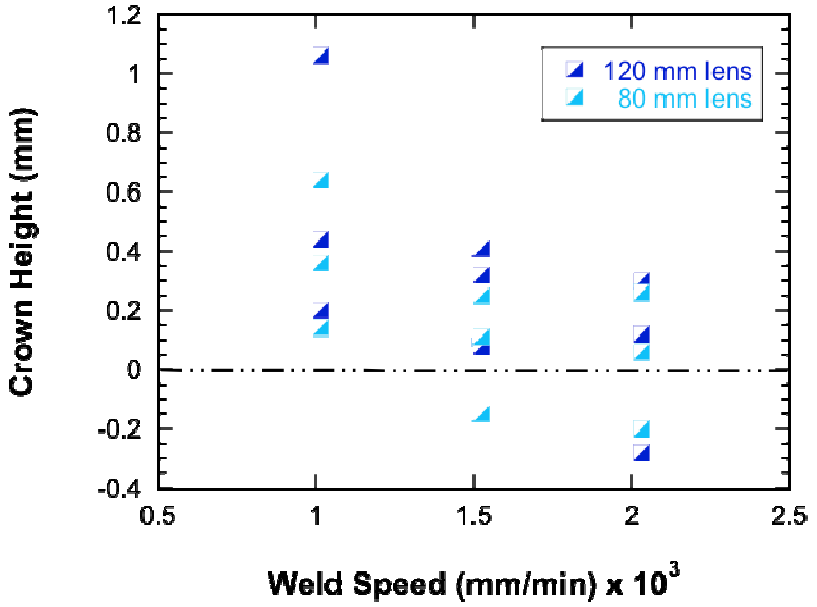

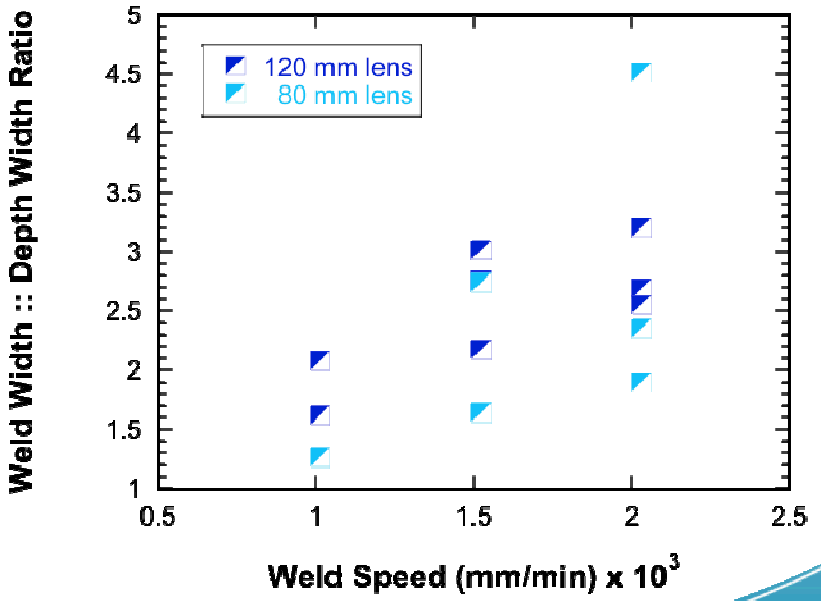

Ultrasonics [UTC]

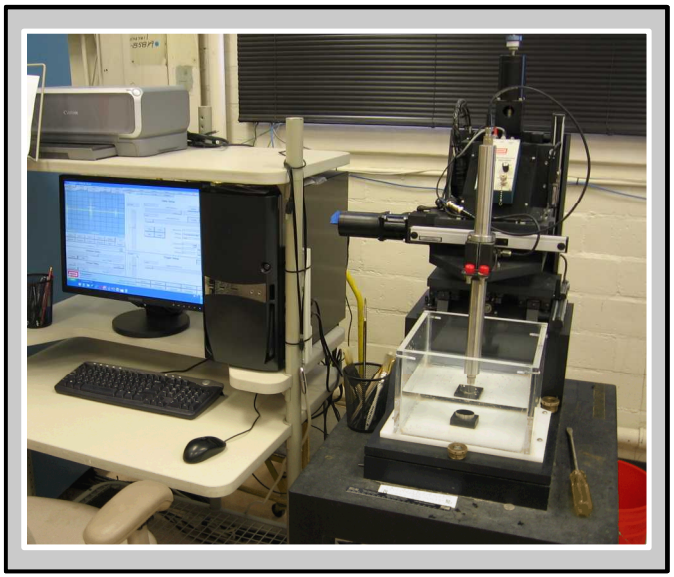

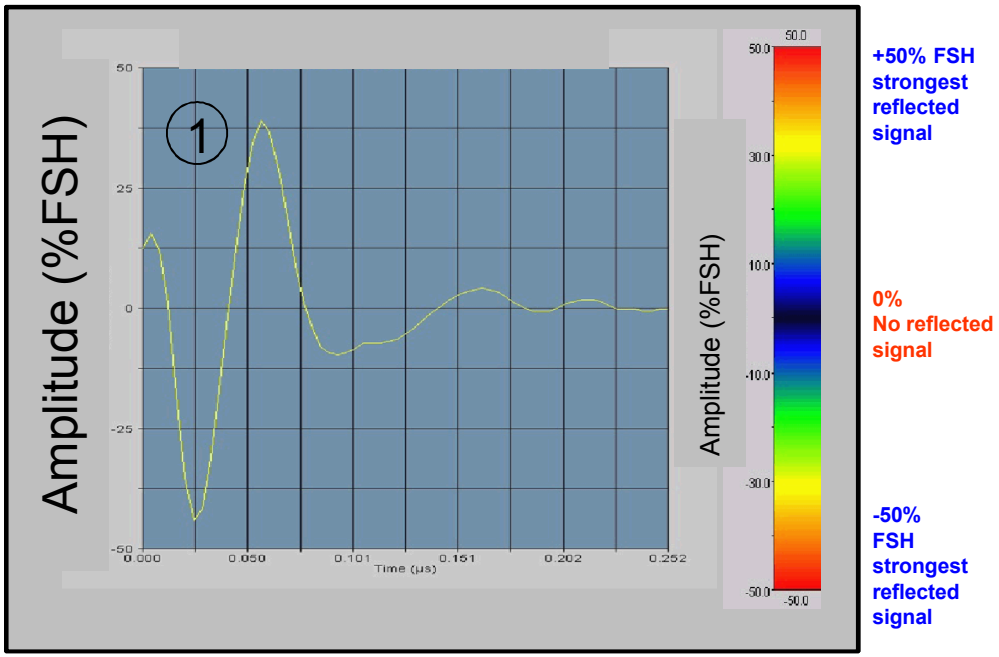

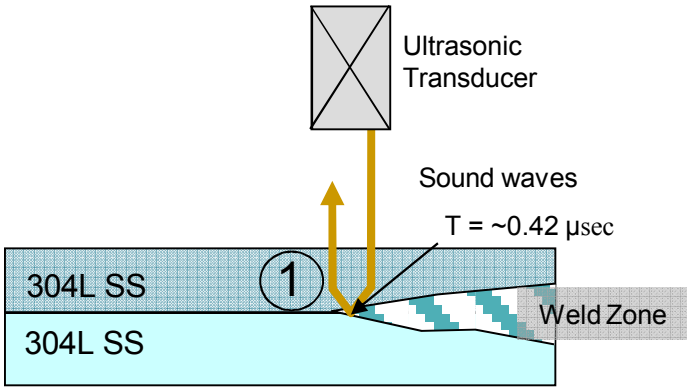

- Sound waves travel across well bonded interfaces better than poorly bonded interfaces.
- Poorly bonded interfaces reflect more sound and produce higher amplitude signals (±50% Full Screen Height). Well bonded interfaces produce a weaker amplitude signal if any (0% FSH)

Ultrasonics [UTC]

80 mm
60”/ min

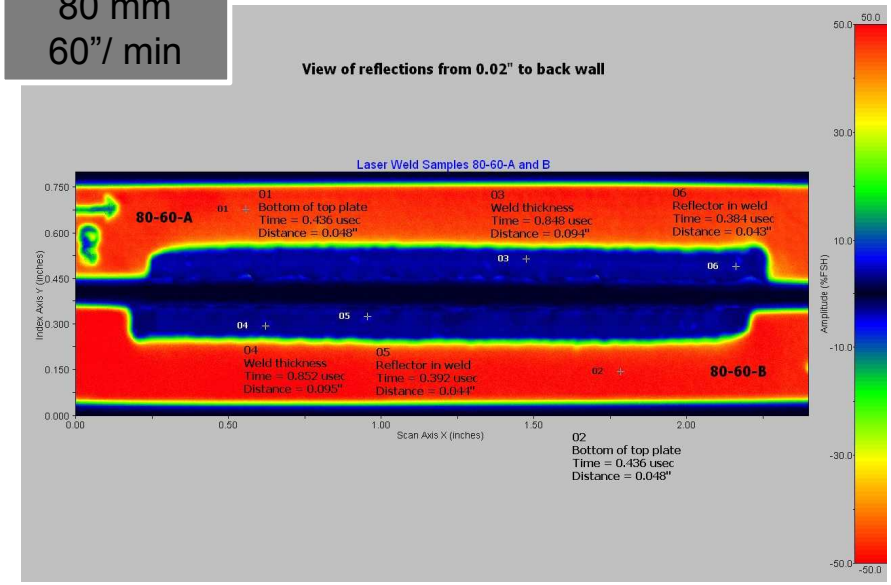

80 mm
40”/ min

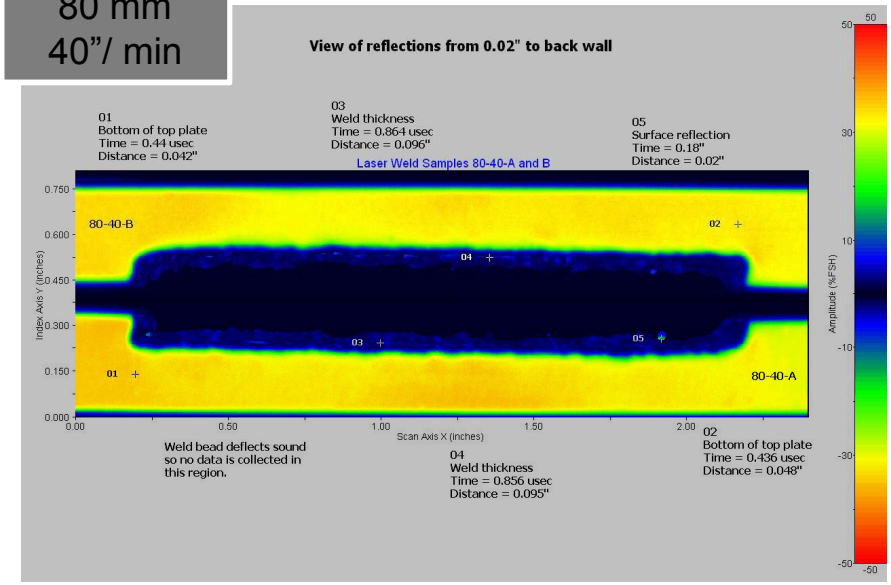

80 mm
80”/ min

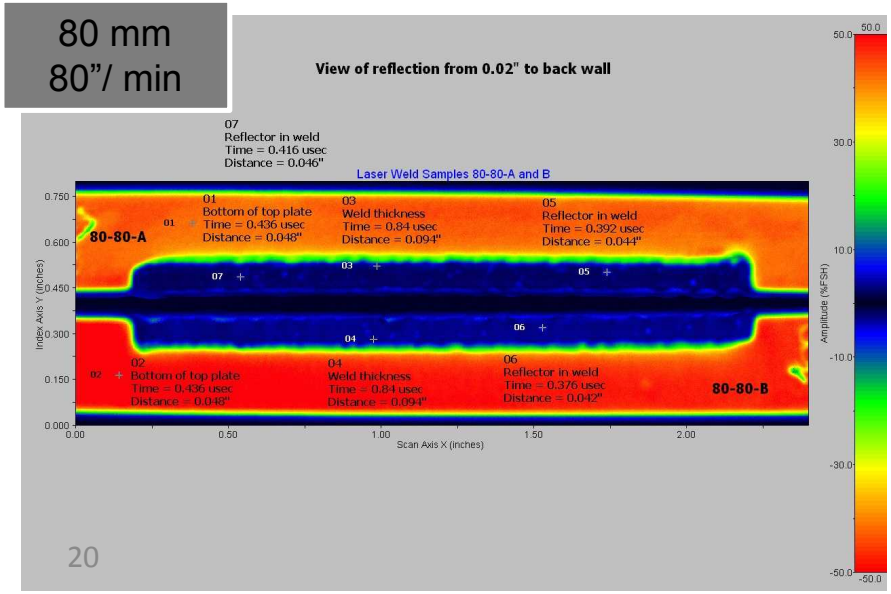

- UTC scans provide resolution of features ~ 0.1 mm^3 and larger
- UTC results are very sensitive to surface character of region of interest
- Surface defects and curvatures deflect transmitted sound waves, which weaken and eliminate the reflected signal in that region.

Ultrasonics [UTC]

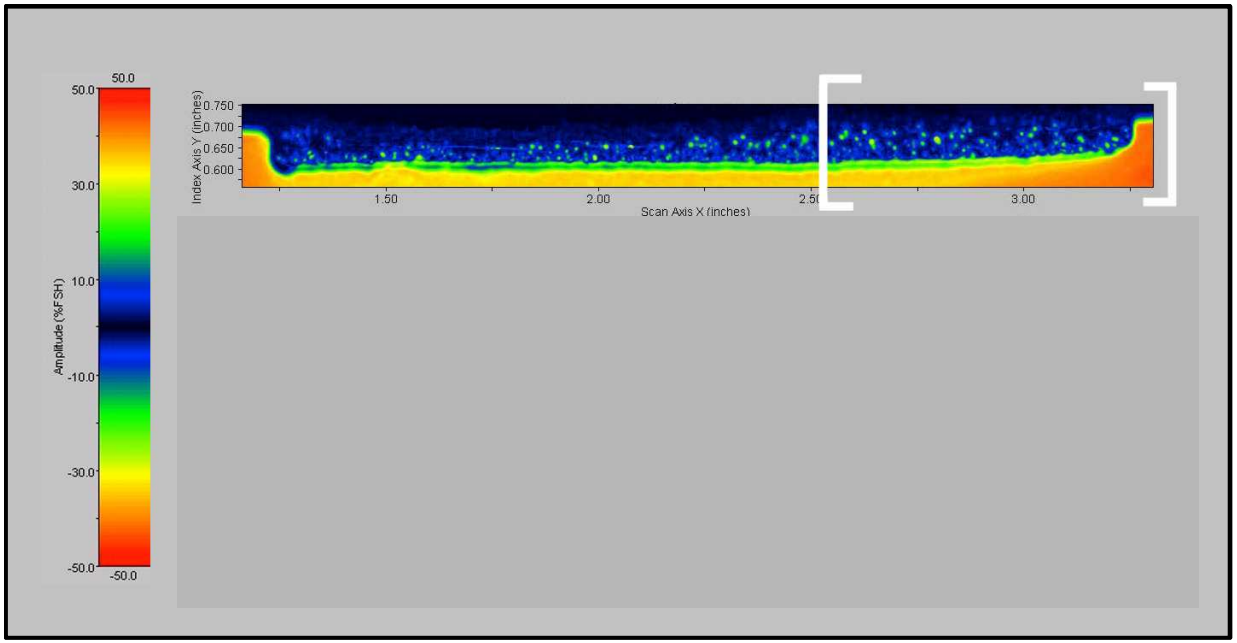

Delesse's Principle

$$V_V = A_A = L_L = P_P$$

V_V = *Volume fraction*
A_A = *Area fraction*
L_L = *Lineal fraction*
P_P = *Point fraction*

E.E. Underwood, Quantitative Stereology, Addison Wesley, (1970)
ASM Handbook, Vol. 9:, Metallography and Microstructures, ASM Intl. (2004)

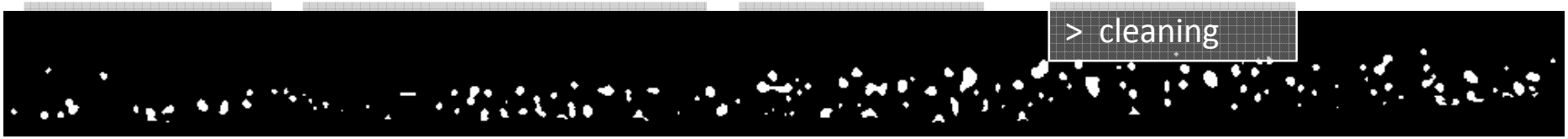

3.67% void fraction

Delesse's Principle only provides accurate relationships provided:
- they are used with statistical uniformity
- 1D, 2D or 3D data represented is true to its dimension

Computed Tomography [µCT]

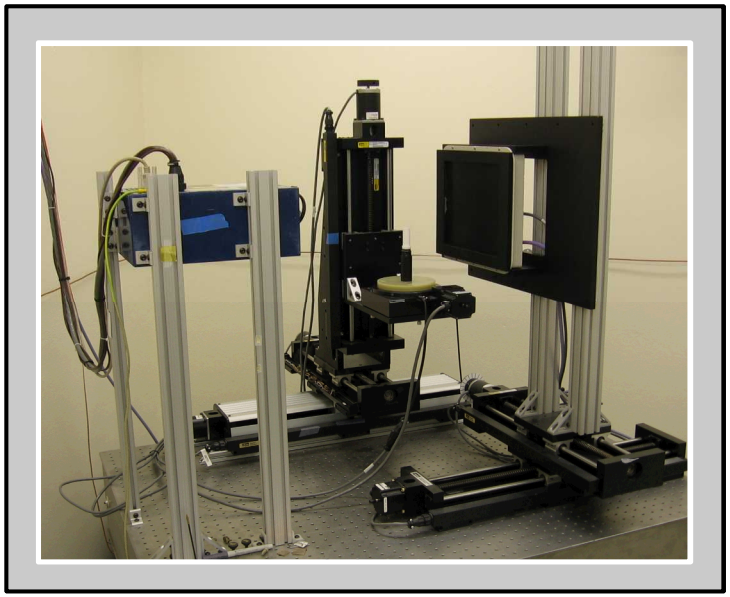

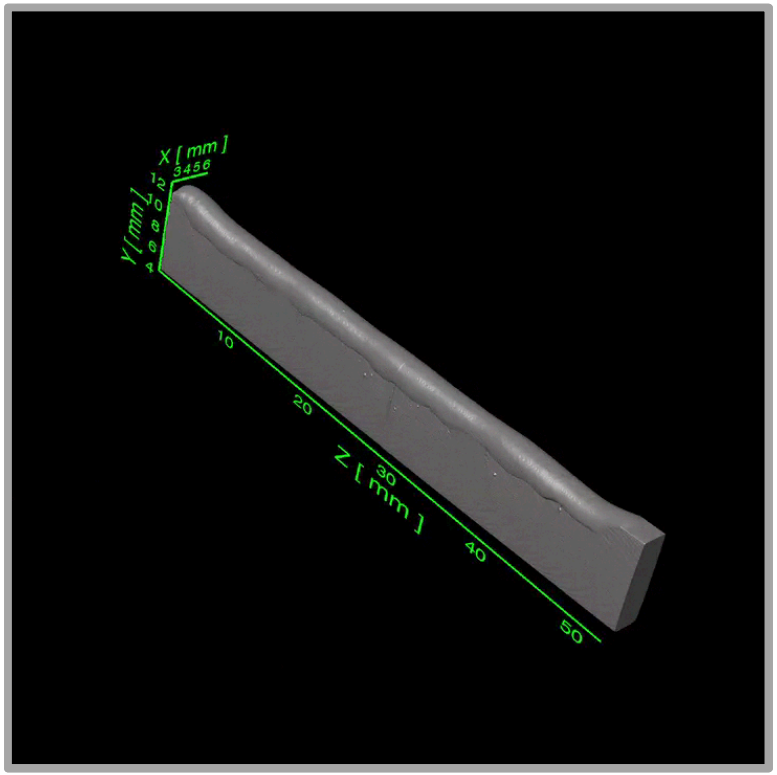

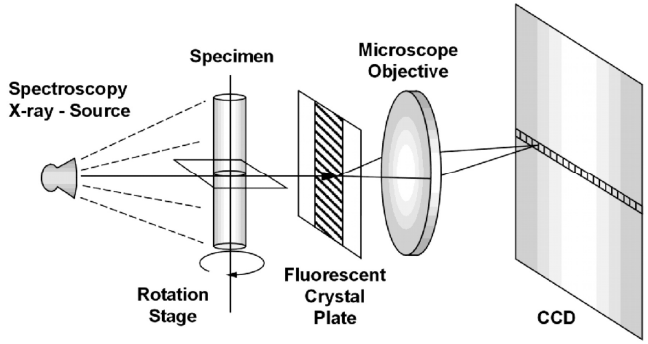

M.D. Bentley, et al. *Am. J. Physiol. Regul. Integr. Comp. Physiol.*,vol. 282, no. 5 (2002)

- Rotation occurs counter clock-wise in front of a fluorescent cesium iodide plate
- 9X magnification yields an effective pixel size of 14 um
- Energy is set to 130KV and 250uA yielding a spot size on the order of 27 um
- Objects 14 um in size can be detected but resolution is not adequate until objects reach 27 um in size

Segmentation & Reconstruction

Image Processing (7 steps)

- Image Shift - loose and initial aligning of images
- Coarse Cropping - remove unnecessary information from images
- Fine Cropping - further remove extraneous data
- Cleaning - remove anomalies and potentials for error from images
- Make Binary - reduce memory needed to process images and simplify stacking
- Set Size - establish size for all images based on largest image in stack
- Size Reduction - resize all images by a uniform scaling factor to allow for practical manipulation of data

Reconstruction & Analysis

- Stack† - create 3-dimensional volume
- Visualize Stack† - use GUI to interact with and survey volume in 3-D
- Additional Scripts - written to return specific values and measures desired

†*IDL code courtesy of D. Rowenhorst of NRL*

µComputed Tomography

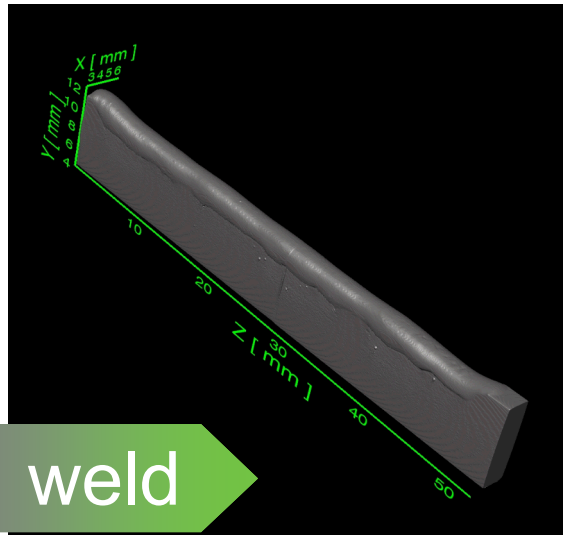

weld

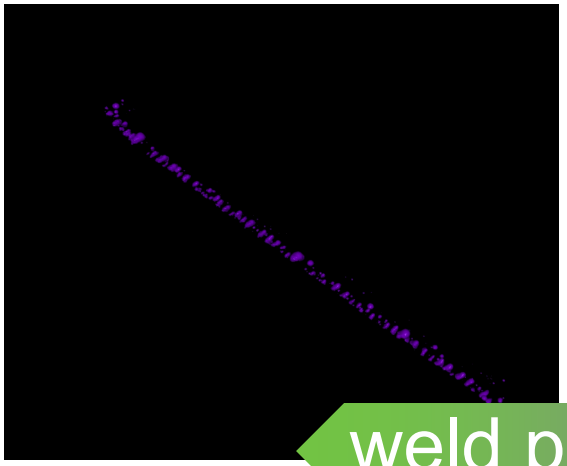

weld porosity

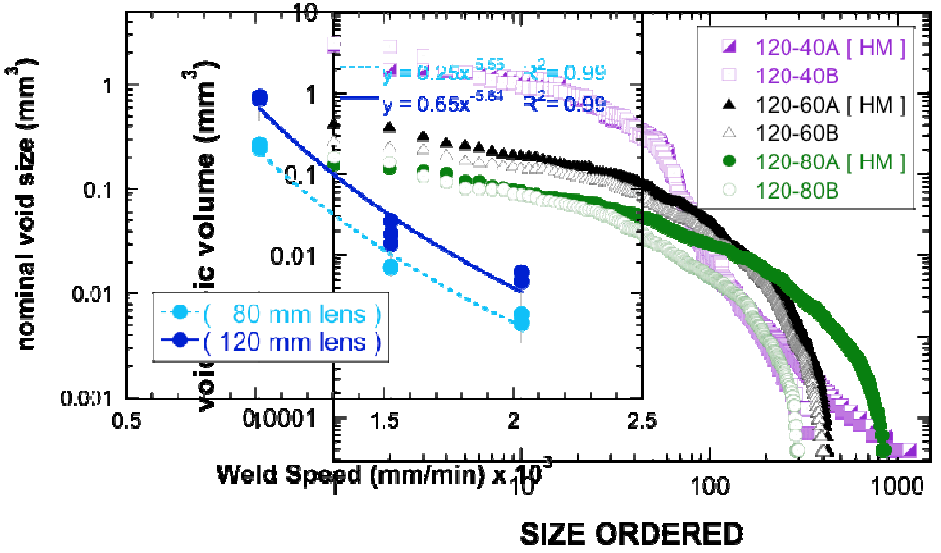

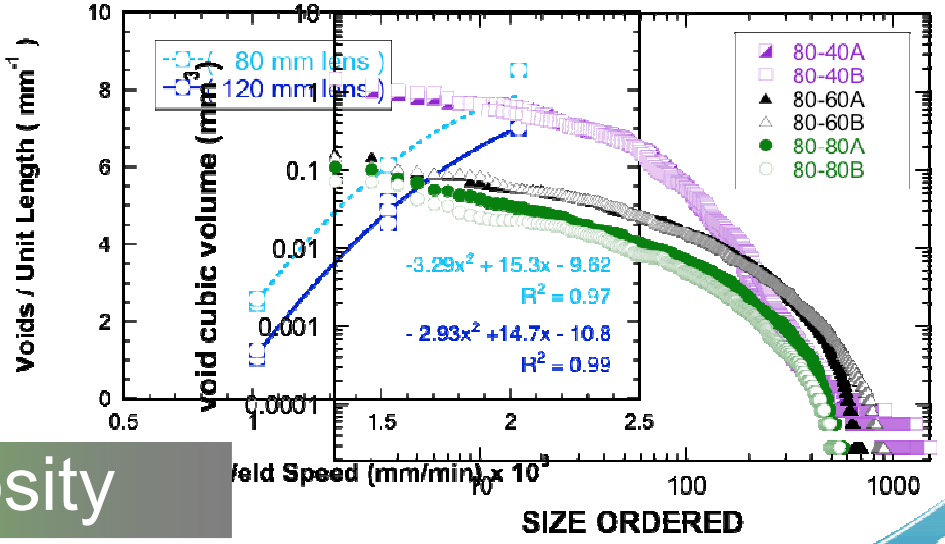

Sandia National Laboratories

µComputed Tomography

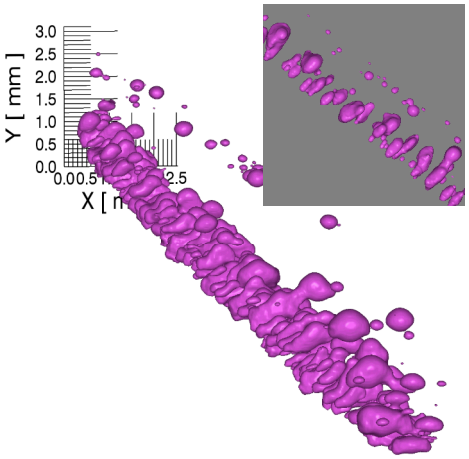

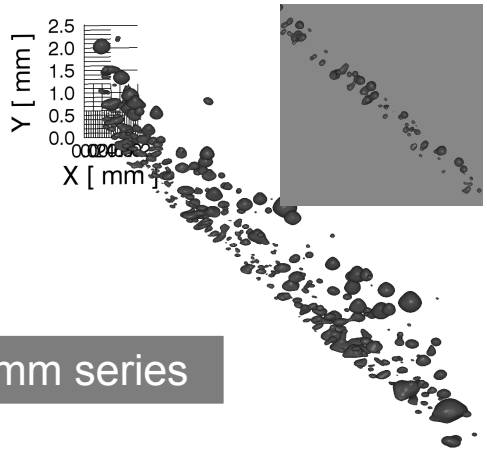

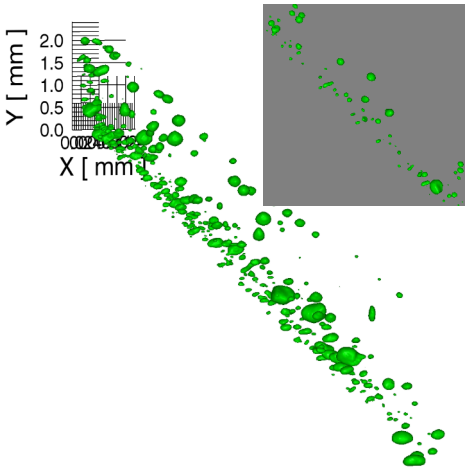

80 mm series

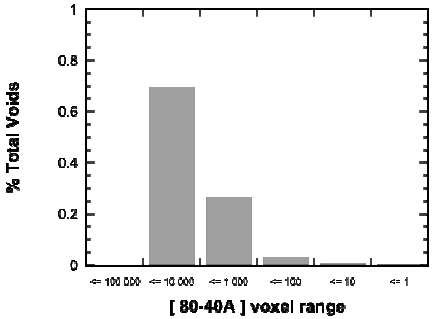

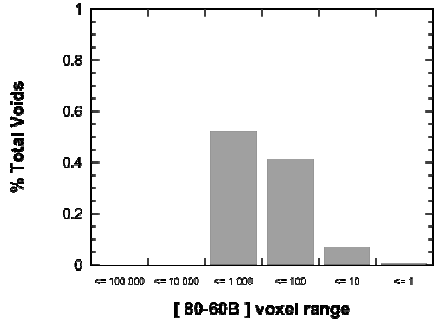

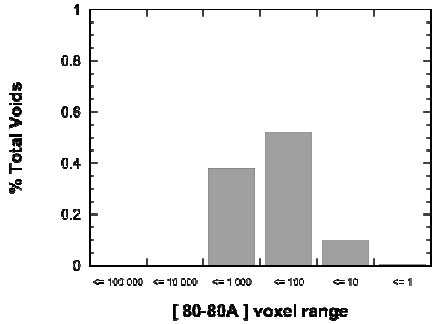

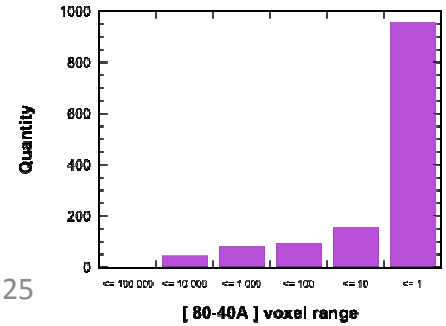

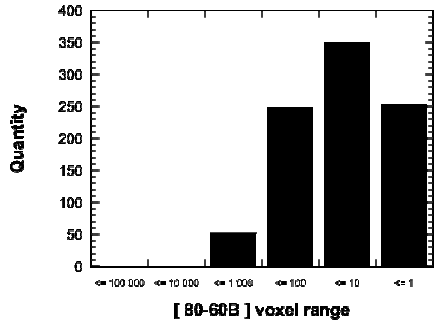

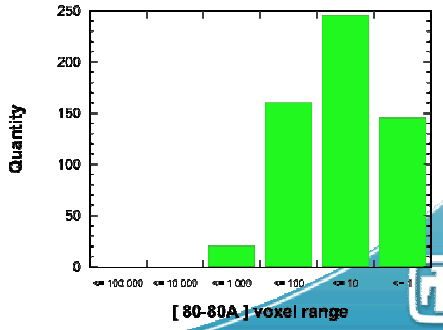

µComputed Tomography

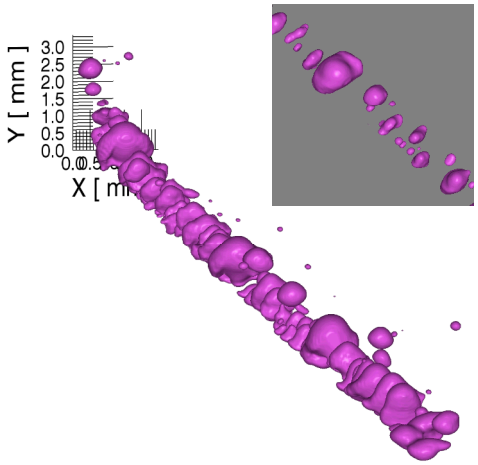

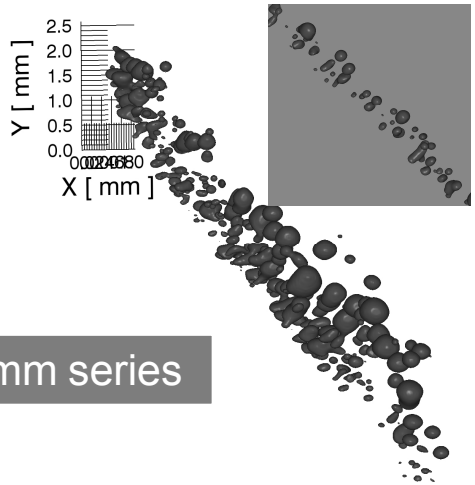

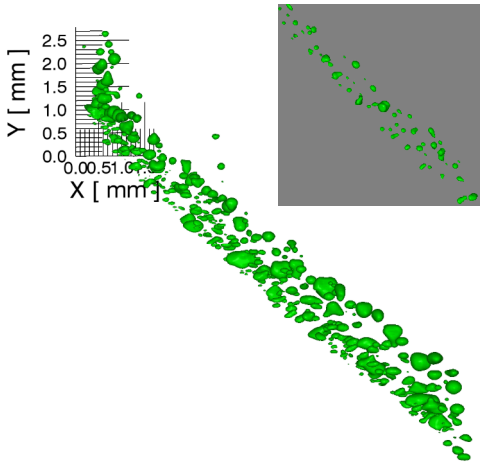

120 mm series

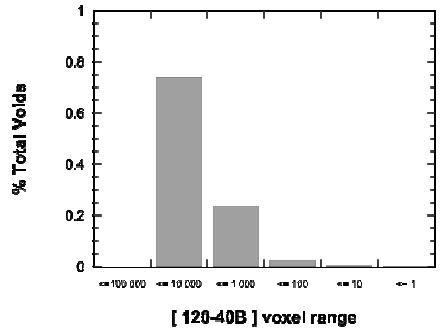

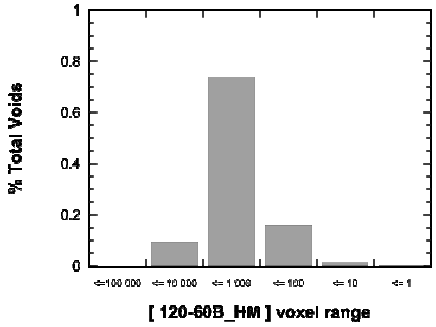

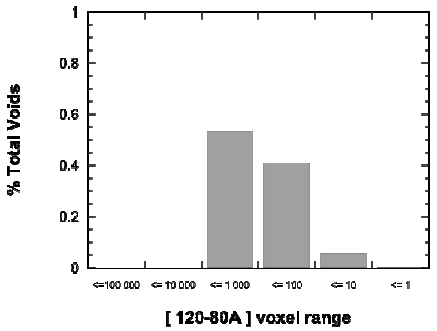

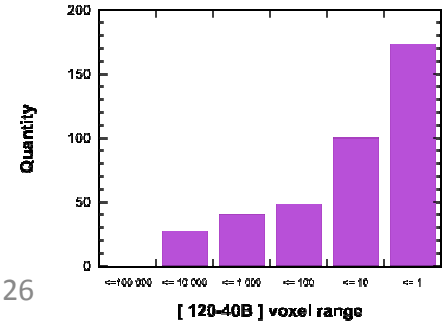

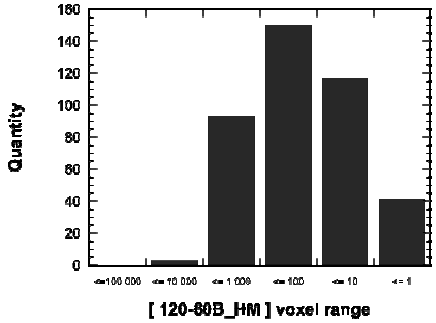

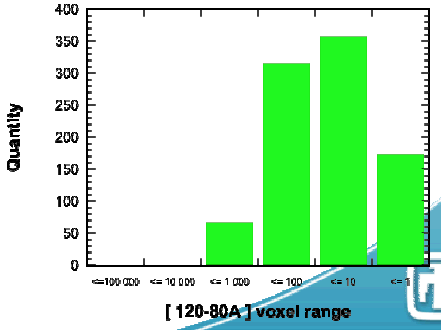

Sandia National Laboratories

µComputed Tomography

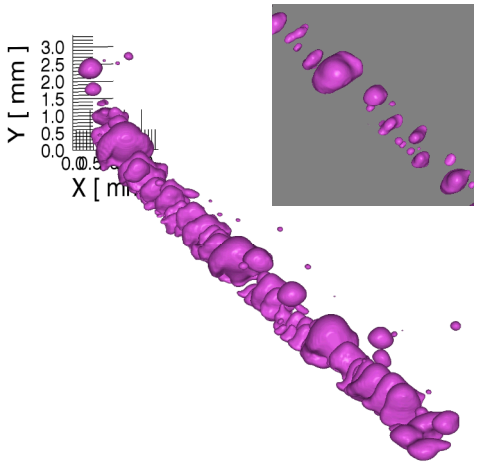

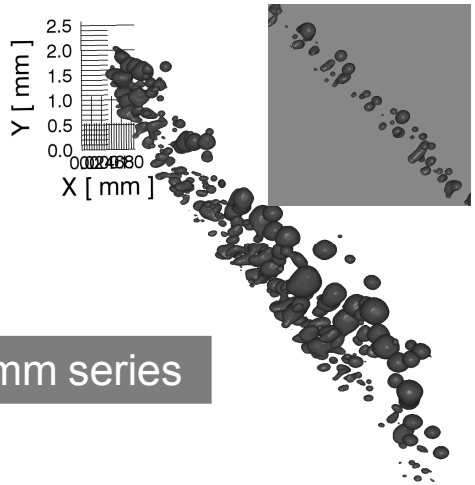

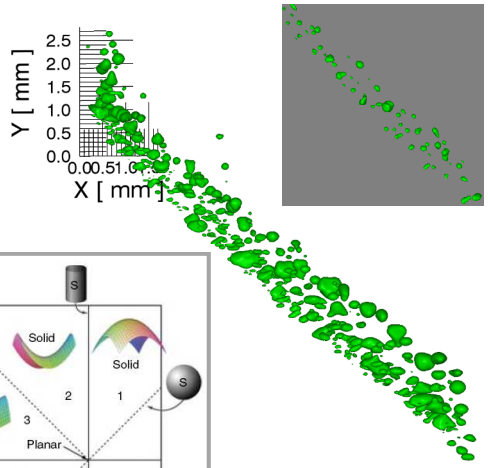

120 mm series

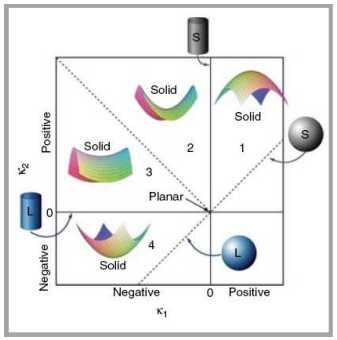

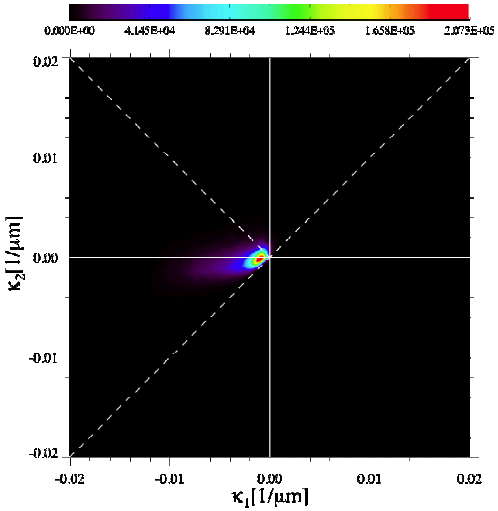

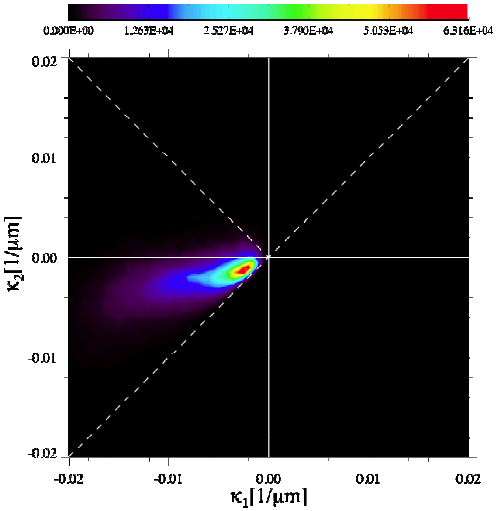

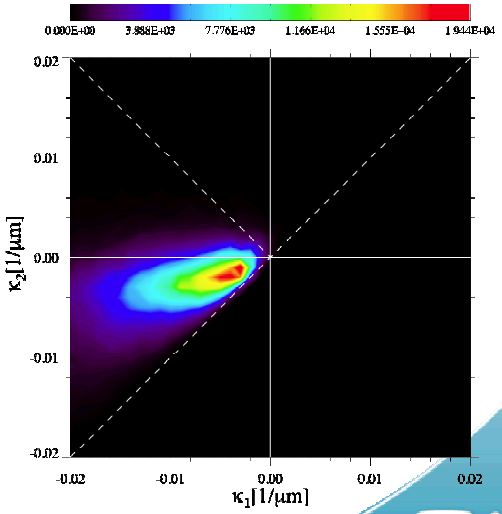

Sandia National Laboratories

Why Study Microstructure in 3D?

- Typical optical & electron microscopy techniques which view 2-Dimensional sections and are inadequate for determining accurate internal 3-Dimensional microstructure
  - Many mistakes in past literature have been revealed in recent 3D studies

- 3-Dimensional shapes & distributions of morphologies:
  - Strongly influence mechanical & physical properties of materials
  - Critical to the predictive models for mechanical and material response

- Powerful hardware and computer software now exists for 3-Dimensional reconstruction, visualization and analysis

- Importance of 3-Dimensional analysis in materials science is now well known and becoming increasingly documented
  - (*e.g. Scripta Materiala,* 2006, vol. 55, no. 1)
  - *(e.g. JOM,* 2006*,* vol. 58, no. 12)
  - (*e.g. MRS Bulletin*, 2008 vol. 33, no. 6)

Summary

- UT scans are useful in identifying bonding gaps, depths of penetration and qualitative estimates of porosity in welds
- MS provides useful information regarding size, shape and relative weld dimensions that can be directly related to processing parameters
- Over the range of parameters examined, increases in weld speed result in an increase in weld width :: depth width ratio and resultant crown heights
- µCT provides a relatively rapid means to gain full 3d evaluations of weld porosity down to a resolution of 27 μm^3
- Across all welds examined, most frequently occurring void sizes constitute less than 10% of the total voided space
- At increasing weld speeds, characteristic porosity curvature transitions from large singular ellipsoids to more uniformly distributed spheres

Future Work

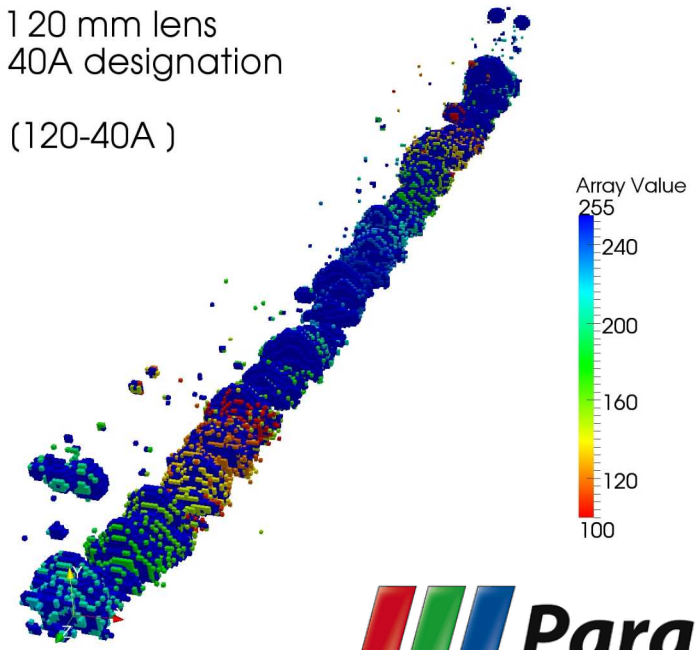

visualization of 3d weld porosity from IDL™ to ParaView

(left: colorized images denote minor adjustments to void edges from downsizing dataset in IDL before passing to Paraview)

ParaView
Parallel Visualization Application

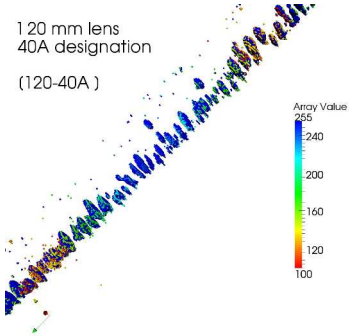

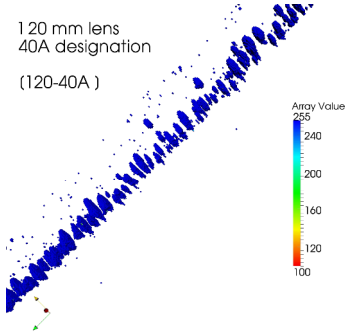

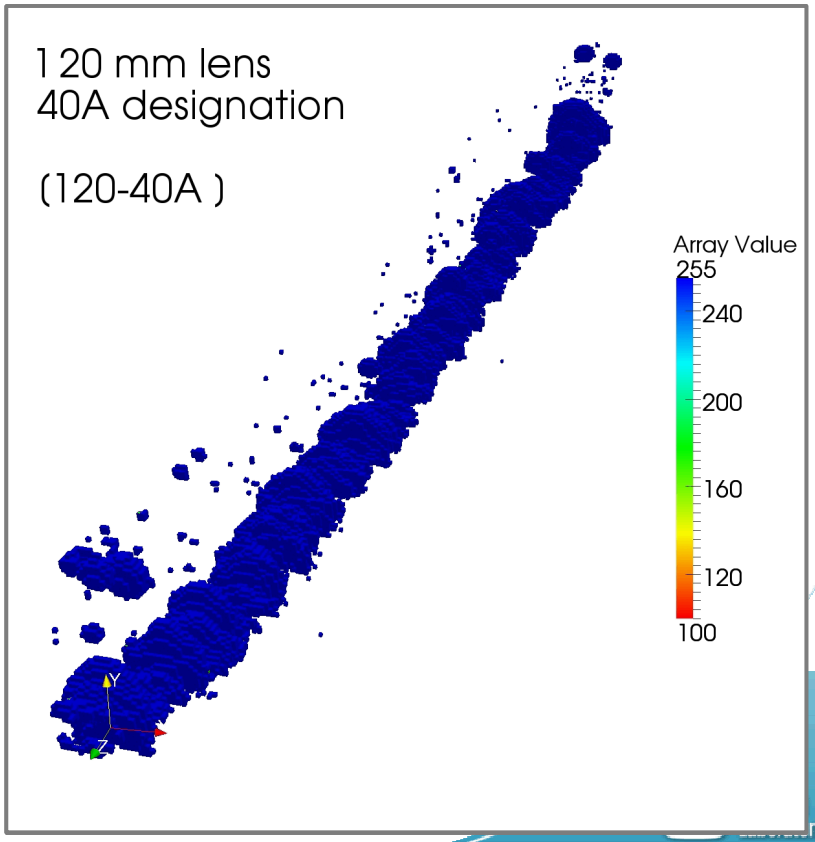

Future Work

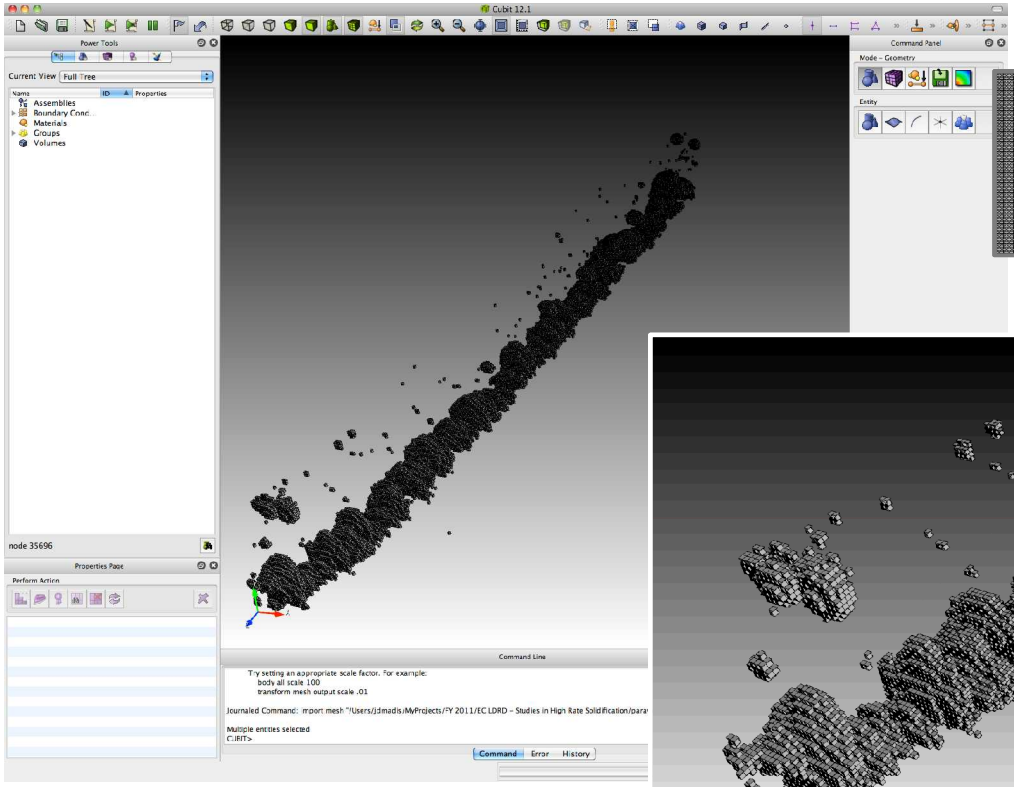

mesh generation of 3d weld porosity in CUBIT

((preliminary export as exodus II file)

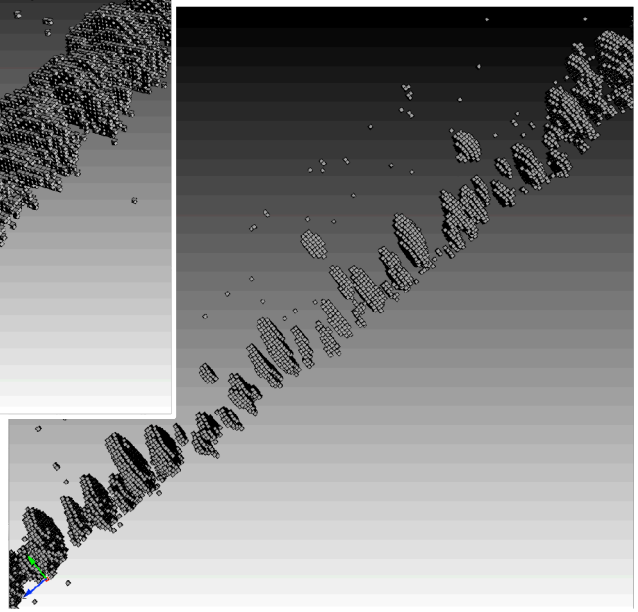

CUBIT 12.1

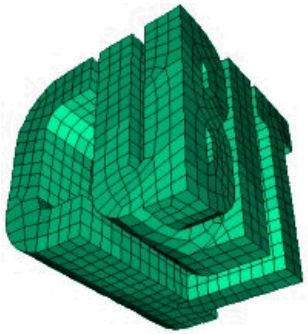

Questions